

Bradykinin postconditioning protects rat hippocampal neurons after restoration of spontaneous circulation following cardiac arrest via activation of the AMPK/mTOR signaling pathway

<https://doi.org/10.4103/1673-5374.337049>

Date of submission: May 17, 2021

Date of decision: August 8, 2021

Date of acceptance: December 29, 2021

Date of web publication: February 28, 2022

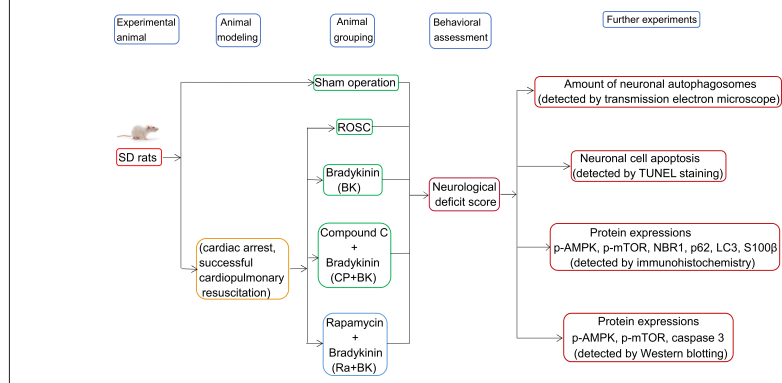
Shi-Rong Lin^{1, 2, 3, 4, 5}, Qing-Ming Lin^{1, 3, 4, 5}, Yu-Jia Lin¹, Xin Qian^{1, 3, 4, 5},
Xiao-Ping Wang^{1, 3, 4, 5}, Zheng Gong^{1, 3, 4, 5}, Feng Chen^{1, 3, 4, 5, *}, Bin Song^{6, 7, 8, *}

From the Contents

Introduction	2232
Materials and Methods	2233
Results	2234
Discussion	2235

Graphical Abstract

Effects of bradykinin postconditioning on hippocampal neurons after restoration of spontaneous circulation following cardiac arrest



Abstract

Bradykinin (BK) is an active component of the kallikrein-kinin system that has been shown to have cardioprotective and neuroprotective effects. We previously showed that BK postconditioning strongly protects rat hippocampal neurons upon restoration of spontaneous circulation (ROSC) after cardiac arrest. However, the precise mechanism underlying this process remains poorly understood. In this study, we treated a rat model of ROSC after cardiac arrest (induced by asphyxiation) with 150 µg/kg BK via intraperitoneal injection 48 hours after ROSC following cardiac arrest. We found that BK postconditioning effectively promoted the recovery of rat neurological function after ROSC following cardiac arrest, increased the amount of autophagosomes in the hippocampal tissue, inhibited neuronal cell apoptosis, up-regulated the expression of autophagy-related proteins LC3 and NBR1 and down-regulated p62, inhibited the expression of the brain injury marker S100β and apoptosis-related protein caspase-3, and affected the expression of adenosine monophosphate-activated protein kinase/mechanistic target of rapamycin pathway-related proteins. Adenosine monophosphate-activated protein kinase inhibitor compound C clearly inhibited BK-mediated activation of autophagy in rats after ROSC following cardiac arrest, which aggravated the injury caused by ROSC. The mechanistic target of rapamycin inhibitor rapamycin enhanced the protective effects of BK by stimulating autophagy. Our findings suggest that BK postconditioning protects against injury caused by ROSC through activating the adenosine monophosphate-activated protein kinase/mechanistic target of the rapamycin pathway.

Key Words: autophagy; bradykinin; cardiac arrest; cardiopulmonary resuscitation; compound C; hippocampus; neuron; rapamycin; restoration of spontaneous circulation

Introduction

Cardiac arrest (CA) is a critical clinical event in which the heart suddenly stops beating (Wallmuller et al., 2012; Perman et al., 2016; Radeschi et al., 2017). CA has a global annual incidence of 20–140/100,000 (Abelairas-Gómez et al., 2019; Andersen et al., 2019). Although advances in cardiopulmonary resuscitation (CPR) technology have enabled 25–40% of patients to recover after restoration of spontaneous circulation (ROSC), those who do survive can suffer substantial brain damage, including neuronal necrosis, apoptosis, and inflammation (Elmer and Callaway, 2017; Nolan, 2017; Twhig et al., 2019).

Bradykinin (BK) is an active component of the kallikrein-kinin system. It is also the most bioactive kinin in mammals and is primarily hydrolyzed into inactive

substances by angiotensin-converting enzyme (also known as kininase II). BK is also an immune/inflammatory polypeptide that has a number of functions: it can cause pain, inflammation, vasodilation, and smooth muscle contraction and increase vascular permeability (Sharma and Al-Sherif, 2006; Paterson et al., 2013; Virych et al., 2017). Abnormal BK expression has been linked to a variety of cardiovascular diseases, including hypertension, myocardial infarction, and heart failure (Gunaruwan et al., 2009; Sharma, 2009; Qu et al., 2015). Therefore, kinin receptor knockout, kinin receptor analogs, kallikrein analogs, and kallikrein transgenic methods play an essential role in the treatment of cardiovascular disease (Olson et al., 2009; Roman-Campos et al., 2010). BK also has a protective effect on nerve function (Martins et al., 2012). A previous study found that supplementation with BK during cardioplegia improves the anti-apoptotic protein profile and reduces cardiomyocyte

¹Provincial College of Clinical Medicine, Fujian Medical University, Fuzhou, Fujian Province, China; ²Department of Emergency, Fujian Provincial Hospital South Branch, Fuzhou, Fujian Province, China; ³Department of Emergency, Fujian Provincial Hospital, Fuzhou, Fujian Province, China; ⁴Fujian Emergency Medical Center, Fuzhou, Fujian Province, China; ⁵Fujian Provincial Key Laboratory of Emergency Medicine, Fuzhou, Fujian Province, China; ⁶Department of Human Anatomy, School of Basic Medical Sciences, Fujian Medical University, Fuzhou, Fujian Province, China; ⁷Key Laboratory of Brain Aging and Neurodegenerative Diseases of Fujian Province, Fuzhou, Fujian Province, China; ⁸Laboratory of Clinical Applied Anatomy, Fujian Medical University, Fuzhou, Fujian Province, China

*Correspondence to: Feng Chen, MD, Cf9066@126.com; Bin Song, PhD, songbin@fjmu.edu.cn.
<https://orcid.org/0000-0001-9959-482X> (Shi-Rong Lin)

Funding: This study was supported by the Fujian Provincial Health Technology Project of China, No. 2018-CX-16 and Fujian Provincial Hospital Flint Fund Project, No. 2020HSSJ17 (both to SRL).

How to cite this article: Lin SR, Lin QM, Lin YJ, Qian X, Wang XP, Gong Z, Chen F, Song B (2022) Bradykinin postconditioning protects rat hippocampal neurons after restoration of spontaneous circulation following cardiac arrest via activation of the AMPK/mTOR signaling pathway. *Neural Regen Res* 17(10):2232-2237.

apoptosis (Yeh et al., 2010). BK also leads to a remarkable reduction in ischemia-induced neuronal death and has neuroprotective effects against delayed neuronal death in hippocampal CA1 neurons (Danielisová et al., 2009). Liu et al. (2016) confirmed that the BK B2 receptor (B2R) can mediate the mitogen-activated protein kinase/extracellular signal-regulated kinase and adenosine monophosphate-activated protein kinase (AMPK) signaling pathways, as well as promote autophagy under cerebral ischemia stress.

Postconditioning is defined as rapid, intermittent interruptions of blood flow during early reperfusion. Postconditioning relieves various manifestations of reperfusion injury, including endothelial activation and dysfunction, as well as infarction and apoptosis (Zhao and Vinten-Johansen, 2006; Gao et al., 2021; Goebel et al., 2021). Previous studies have demonstrated loss of cardioprotection after delayed postconditioning (Yang et al., 2004). The degree of protection conferred by postconditioning is comparable to that conferred by ischemic preconditioning (Zhao et al., 2003), and, in contrast to preconditioning, which requires previous knowledge of the ischemic event, postconditioning can be used in clinical settings at the onset of reperfusion, such as during angioplasty, cardiac surgery, and transplantation (Vinten-Johansen et al., 2005). Previous research has suggested that ischemic postconditioning can promote autophagy, thereby protecting against ischemia/reperfusion injury, at least partly through activating the neuronal nitric oxide synthase/AMPK/mechanistic target of rapamycin (mTOR) pathway (Hao et al., 2017).

We previously found that BK postconditioning had a clear neuroprotective effect in the context of ROSC following CA in rats (Lin et al., 2015). However, the specific mechanism underlying this effect remains unclear. Therefore, the aim of this study was to explore the mechanism by which BK postconditioning exerts its neuroprotective effects. We hypothesized that BK postconditioning can reduce brain injury caused by ROSC after CA through activation of the AMPK/mTOR signaling pathway and regulation of autophagy- and apoptosis-related protein expression. Compound C, an AMPK inhibitor, and rapamycin, which is an mTOR inhibitor, were used to investigate whether BK can reduce neuronal injury in rats after ROSC by activating the AMPK-mTOR signaling pathway.

Materials and Methods

Ethics statement

This study was approved by and conducted in strict accordance with the guidelines of the Animal Care and Use Committee of Fujian Provincial Hospital of China. Ethical approval was granted on August 21, 2019.

Experimental animals

Forty-seven healthy, adult, male, 9- to 10-week-old, specific pathogen-free Sprague-Dawley rats weighing 350–400 g were purchased from Beijing Vital River Laboratory Animal Technology Co., Ltd., China [license No. SCXK (Jing) 2016-0006]. They were randomly allocated into separate cages and allowed *ad libitum* access to food and water. They were allowed to acclimate to the laboratory environment (22–25°C, 50–60% humidity, standard 12-hour/12-hour light/dark cycle) for 5 days. The rats were fasted for 10 hours (water allowed) before the experiment. Female rats were not included to avoid interference from the estrous cycle (Singh et al., 2011). All experiments were designed and reported according to the Animal Research: Reporting of *In Vivo* Experiments (ARRIVE) guidelines (Percie du Sert et al., 2020).

Animal grouping

The rats were randomly allocated into five groups ($n = 8$ rats/group). After anesthetization via intraperitoneal (IP) injection of sodium pentobarbital (45 mg/kg), the rats underwent a series of invasive procedures, including tracheal intubation and femoral artery catheterization. For the sham operation group (Sham), physiological saline (150 µg/kg) was administered via IP injection 48 hours after the invasive procedures, and no other intervention was performed. Rats subjected to CA and successful CPR were randomly assigned to one of the following groups: ii) ROSC group, IP injection of physiological saline (150 µg/kg) 48 hours after ROSC; iii) BK group, IP injection of BK (150 µg/kg; Cat# 193526; EMD Millipore) 48 hours after ROSC; iv) compound C (CP) + BK group, IP injection of CP (250 µg/kg; Cat# CSN13424; CSNpharm, Inc., Arlington Heights, IL, USA) 30 minutes before asphyxia-induced CA; and v) rapamycin (Ra) + BK group, IP injection of Ra (1 mg/kg; an effective and specific mTOR inhibitor; Cat# 553211; EMD Millipore) 30 minutes before asphyxia-induced CA. BK (150 µg/kg) was administered by IP injection 48 hours after ROSC in the CP + BK and Ra + BK groups.

Animal modeling

Cardiac arrest

CA was induced by asphyxiation, as described previously (Lee et al., 2019; Lu et al., 2020). After anesthetization via IP injection of sodium pentobarbital (45 mg/kg; Cat# P3761; EMD Millipore, Burlington, MA, USA), the rats were placed on the operating table in a supine position. The skin of the neck, chest, and groin area was sterilized and prepared for further steps. The head end of the table was tilted 30° from the horizontal plane. A bright flashlight was used to penetrate through the prepared area of skin on the neck. The tongue was lifted with gauze in the left hand, and the endotracheal intubation catheter inserted with a needle core was held in the right hand. The catheter was inserted into the trachea, then the needle core was withdrawn quickly, and the catheter was secured to the rat mandible with a suture needle (Additional

Figure 1A). The left femoral artery was separated, the blood flow was blocked with ophthalmic forceps, and the distal end was ligated. A small incision was made in the proximal end with ophthalmic scissors, and a PE50 heparinized tube (Becton Dickinson Co., Franklin Lakes, NJ, USA) was inserted at a depth of 3–4 cm (Additional Figure 1B). The end of the PE50 tube was connected to an arterial pressure measuring device to continuously monitor mean arterial pressure. The electrodes were placed on the upper and lower limbs to continuously monitor electrocardiogram (ECG) changes (lead II) (BL-420S biological function experimental system, Chengdu Techman Software Co., Ltd., Sichuan, China). Once the rat was awake, the baseline of each physiological parameter was recorded. Rocuronium (0.1 mL/100 g; Cat# Y0000527; EMD Millipore) was injected into a three-way valve, and the tracheal intubation site was blocked with a syringe. The criteria for inducing CA were as follows (Lin et al., 2015, 2020): i) the mean blood pressure decreased rapidly to < 20 mmHg after rocuronium injection; ii) the arterial pulse waveform disappeared on blood pressure monitoring; and iii) the ECG waveform showed ventricular fibrillation or pulseless electrical activity on ECG monitoring.

For the rats in the Sham group, after anesthesia, they underwent a series of invasive procedures, including tracheal intubation and femoral artery catheterization, and no other intervention was performed.

Cardiopulmonary resuscitation

The rat limbs and head were fixed in position, and the chest was fully exposed. The lower part of the sternum was marked as the compression site with a marker. The syringe was removed 6 minutes after CA. Pure oxygen mechanical ventilation (respiratory rate: 100 times/min, tidal volume: 0.6 mL/100 g, inhalation/exhalation ratio: 1:1) was administered. Hands-only external chest compressions were performed at 200 times/min. The compression depth was 1/3 of the anteroposterior chest diameter. A total of 0.1 mL epinephrine (Cat# E4642; EMD Millipore) was administered 2 minutes after the compression. Indicators for ROSC (He et al., 2011; Lin et al., 2020) included recovery of supraventricular heart rhythm and mean arterial pressure > 60 mmHg, which was maintained for > 10 minutes. The rats were not anesthetized during CPR.

Management of rats with successful resuscitation

A total of 32 rats (~80%) were successfully resuscitated. Mechanical ventilation was maintained for 2 hours. The ECG and mean arterial pressure measurements were continued for 1 hour. All catheters were removed under anesthesia. Then, the skin was sutured and sterilized with iodophor (Cat# 1234; Shangqiu Huachen Trading Co., Ltd., Zhengzhou, Henan Province, China), and the rats were given an IP injection of penicillin (100,000 units; Cat# P0389; EMD Millipore) each day for 3 days. After 3 days of observation, the rats were scored for neurological function using the neurological deficit scale (NDS) by two observers (YJL and ZG) who were blinded to the animal grouping; the scores from the two assessors were averaged. The NDS, which assesses seven main parameters (general behavior, brainstem reflex, movement, sensory, motor, behavior, and seizures) is widely used to evaluate the neurological function of rats after ROSC. On a scale of 0 to 80, 0 indicates brain death, while 80 indicates no neurological deficit (Additional Table 1) (Geocadin et al., 2000; Jia et al., 2006).

Detection of neuronal autophagosomes by transmission electron microscopy

Three days after ROSC, the rats were anesthetized by IP injection of 1% sodium pentobarbital (45 mg/kg), followed by left ventricular perfusion and fixation with physiological saline and paraformaldehyde, after which the brain was removed. The hippocampal tissue was isolated and fixed for 2 hours at 4°C in 2.5% glutaraldehyde (Cat# G5882; EMD Millipore). Then, the tissue was washed with precooled phosphate buffer saline (PBS) (three times), and dehydrated in 50%, 70%, 80%, 90%, and 100% ethanol for 10 minutes each, and in acetone for 10 minutes. The dehydrated tissues were incubated in pure embedding solution overnight at room temperature, then placed in embedding molds and heated in an oven at 60°C to solidify the embedding agent. The paraffin-embedded tissues were sliced with an ultramicrotome (UC7; Leica Microsystems, Inc., Wetzlar, Germany) to a thickness of 70–100 nm. The sections were double-stained for 20 minutes at room temperature with 2% uranyl acetate (Cat# SPI-02624; Hede Biotechnology Co., Ltd., Guangdong, China), then for 5 minutes with lead citrate (Cat# HD17800; Hede Biotechnology Co., Ltd.). Images of the neuronal autophagosomes were captured using a transmission electron microscope (Tecna Spirit T12; FEI; Thermo Fisher Scientific, Inc.).

Apoptosis detection by terminal deoxynucleotidyl transferase dUTP nick end-labeling staining

The hippocampal tissue sections were heated at 65°C for 2 hours. Then, the tissue sections were dewaxed, hydrated, and placed in xylene for 10 minutes at room temperature. The xylene was then replaced with fresh xylene, and the sections were allowed to incubate for another 10 minutes. Subsequently, the sections were placed in 100% (twice), 95%, and 80% ethanol, followed by purified water, for 5 minutes each, and then into a wet box, to which a proteinase K working solution (50 µg/mL per sample) was added, and the samples were allowed to react at 37°C for 30 minutes. Then, they were thoroughly washed for 5 minutes with PBS (three times), and the excess PBS was absorbed with absorbent paper. Each slide was treated with a sufficient amount of terminal deoxynucleotidyl transferase dUTP nick-end labeling (TUNEL) detection solution (Cat# C1088; Beyotime Institute of Biotechnology,

Shanghai, China) and incubated in the dark at 45°C for 2 hours. The excess solution was washed off for 5 minutes with PBS (three times). 4',6-Diamidino-2-phenylindole (Cat# abs47047616; Absin Bioscience Inc., Shanghai, China) was added dropwise, and the slides were incubated in the dark at room temperature for 5 minutes. Nuclear staining was performed, and excess 4',6-diamidino-2-phenylindole was rinsed off with PBS. The remaining liquid on the glass slide was wicked off with absorbent paper. Drops of anti-fade fluorescence mounting medium were applied. The images were examined and captured using a fluorescence microscope (CKX53; Olympus Corporation, Shinjuku, Tokyo, Japan) at 400× magnification. The TUNEL-positive cells in each group were counted with Image-Pro Plus software (v5.1; Media Cybernetics, Inc., Rockville, MD, USA). In total, three fields of view per section (at least three sections/rat) were randomly selected for quantification, before the mean value was taken.

Immunohistochemistry

The AMPK/mTOR signaling pathway, autophagy-related proteins, and brain injury marker expression were detected by immunohistochemistry. The prepared hippocampal tissue sections were dewaxed, hydrated, and placed in 100% (twice), 95%, and 80% ethanol, followed by purified water for 5 minutes, with each step carried out at room temperature. Citrate buffer (Cat# C1010; Beijing Solarbio Science & Technology Co., Ltd., Beijing, China) was added for antigen retrieval. After washing with PBS (three times), 5% bovine serum albumin (Cat# A8020; Beijing Solarbio Science & Technology Co., Ltd.) was added, and blocking was performed at 37°C for 30 minutes. The diluted primary antibodies [S100 calcium-binding protein B (S100β, a brain injury marker; 1:100; rabbit; Cat# ab52642, RRID: AB_882426; Abcam Co., Cambridge, MA, USA), phosphorylated mTOR (p-mTOR; 1:100; rabbit; Cat# ab109268, RRID: AB_10888105; Abcam Co.), neighbor of breast cancer 1 gene (NBR1; an autophagy-related protein; 1:100; rabbit; Cat# DF12049, RRID: AB_2844854; Abcam Co.), microtubule-associated protein 1 light chain 3 (LC3) I/II (an autophagy-related protein; 1:100; rabbit; Cat# AF5402, RRID: AB_2837886; Affinity Biosciences, Cincinnati, OH, USA), phosphorylated AMPK (p-AMPK; 1:100; rabbit; Cat# AF3423, RRID: AB_2834865; Affinity Biosciences), and p62 (an autophagy-related protein; 1:100; rabbit; Cat# 18420-1-AP, RRID: AB_10694431; ProteinTech Group, Inc., Rosemont, IL, USA)] were then added, and the sections were incubated in a wet box overnight at 4°C. Subsequently, the wet box was allowed to sit at room temperature for 45 minutes. The slides were then soaked in PBS for 5 minutes (three times). Incubation with goat anti-rabbit IgG heavy and light chain (H + L) horseradish peroxidase-conjugated (1:100; Cat# ZB-2301, RRID: AB_2747412; ZSGB-BIO; OriGene Technologies, Inc., Beijing, China) was performed at 37°C for 30 minutes. Then, the sections were thoroughly rinsed with PBS, the color was developed with 3,3'-diaminobenzidine (Cat# CW0125; CoWin Biosciences, Beijing, China) for 7 minutes at room temperature, and the slides were then washed with PBS for 1 minute and counterstained with hematoxylin (Cat# AR1180-1; Wuhan Boster Biological Technology, Ltd., Wuhan, China) for 3 minutes at room temperature. Subsequently, hydrochloric acid differentiation and bluing were performed. Then, the slides were rinsed for 1 minute with tap water, dehydrated, cleared, mounted, and examined under a light microscope (CX41; Olympus Corporation, Tokyo, Japan). A total of four fields of view at 400× magnification were analyzed. Images were captured, the JEOR 801D morphological image analysis system software (v6.0; Nanjing Jieda Technology Co., Ltd., Nanjing, China) was used to determine the integrated optical density (IOD) of three images, and the mean value was taken.

Western blot assay

The AMPK/mTOR signaling pathway and apoptosis-related protein expression were detected by Western blot assay. The rat hippocampal tissue (0.2 g) was isolated and ground into powder in liquid nitrogen. The powder was then ground further with the addition of radioimmunoprecipitation assay lysis buffer (Cat# C1053; Applygen Technologies, Inc., Beijing, China). Next, the tissue homogenate was transferred to Eppendorf tubes and kept on ice for 30 minutes. After centrifugation at 13,523 × g for 15 minutes at 4°C, the supernatant was carefully aspirated to obtain total protein. The protein concentration was quantified using a bicinchoninic acid kit (Cat# CW00145; CoWin Biosciences). Total protein was denatured at 100°C for 5 minutes, loaded (40 μg/lane), and subjected to sodium dodecyl sulfate-polyacrylamide gel electrophoresis for 2 hours. This was followed by transfer to a PVDF membrane at 300 mA constant current for 80 minutes. Incubation with the primary antibodies (p-AMPK [1:1000; rabbit; Cat# 2535, RRID: AB_331250; Cell Signaling Technology, Inc., Danvers, MA, USA], p-mTOR [1:1000; rabbit; Cat# ab109268, RRID: AB_10888105; Abcam Co.], caspase-3 [an apoptosis-related protein; 1:500; rabbit; Cat# ab44976, RRID: AB_868674; Abcam Co.], and glyceraldehyde 3-phosphate dehydrogenase [1:2000; mouse; Cat# TA-08, RRID: AB_2747414; ZSGB-BIO; OriGene Technologies, Inc.]) was carried out at 4°C overnight, followed by incubation with goat anti-mouse IgG (H + L) horseradish peroxidase-conjugated secondary antibody (for internal reference; 1:2000; Cat# ZB-2305, RRID: AB_2747415; ZSGB-BIO; OriGene Technologies, Inc.) and goat anti-rabbit IgG (H + L) horseradish peroxidase-conjugated secondary antibody (for target protein; 1:2000; Cat# ZB-2301, RRID: AB_2747412; ZSGB-BIO; OriGene Technologies, Inc.) at room temperature for 2 hours. Enhanced chemiluminescence reagent (Cat# RJ239676; Thermo Fisher Scientific, Inc., Waltham, MA, USA) was added dropwise onto the membrane, which was then exposed using a gel imaging system (ChemiDoc™ XRS+; Bio-Rad Laboratories (Shanghai) Co., Ltd., Shanghai, China). The IOD of each band was determined using Image-Pro Plus software. Relative protein expression was normalized to glyceraldehyde 3-phosphate dehydrogenase.

Statistical analysis

The sample size was determined based on the results from our previous study (Lin et al., 2015), in which eight rats per group showed that BK postconditioning could improve neurological function, suggesting that a similar sample size would be appropriate for this study. All assessments were made by observers blinded to the grouping. Graphpad Prism 7 (GraphPad Software, San Diego, CA, USA) was used for statistical analysis and drawing the graphs. All experiments were repeated three times, and the quantitative results are expressed as mean ± standard deviation (SD). One-way analysis of variance (ANOVA) was performed for quantitative numerical comparisons among multiple groups, and Tukey's *post hoc* method was used for pairwise comparisons. The significant difference level was $\alpha = 0.05$.

Results

Bradykinin postconditioning increases the NDS of ROSC rats

Behavioural assessment was performed to determine the effect of BK postconditioning on ROSC rats. As shown in **Figure 1**, the rats in the ROSC group had a significant decrease in NDS compared with those in the Sham group ($P < 0.01$). The rats in the BK group showed a significant increase in NDS compared with that in the ROSC group ($P < 0.05$). The rats in the CP + BK group demonstrated a significant decrease in NDS ($P < 0.05$), while the rats in the Ra + BK group showed a significant increase in NDS compared with that in the BK group ($P < 0.05$). These findings suggest that BK postconditioning can improve the NDS of ROSC rats.

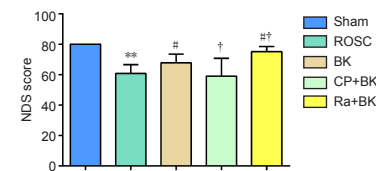


Figure 1 | Effect of bradykinin postconditioning on the NDS score of rats with restoration of spontaneous circulation.

A higher score indicates better neurological function, with a score of 80 indicating no neurological deficit. All data are presented as the mean ± SD ($n = 8$). ** $P < 0.01$, vs. Sham group; # $P < 0.05$, vs. ROSC group; † $P < 0.05$, vs. BK group (one-way analysis of variance followed by Tukey's *post hoc* test). BK: Bradykinin; CP: compound C; NDS: neurological deficit scale; Ra: rapamycin; ROSC: restoration of spontaneous circulation; Sham: sham operation.

Bradykinin postconditioning increases the amount of autophagosomes in the hippocampus of ROSC rats

The amount of autophagosomes in the hippocampus was evaluated to determine the effect of BK postconditioning on neuronal autophagy in ROSC rats. As indicated by the transmission electron microscopy images shown in **Figure 2**, the ROSC group exhibited an increase in the amount of neuronal autophagosomes compared with the Sham group. The BK group exhibited an increase in the amount of neuronal autophagosomes compared with the ROSC group. The amount of neuronal autophagosomes in the CP + BK group remained unchanged, whereas the amount of neuronal autophagosomes in the Ra + BK group was increased compared with that seen in the BK group. These findings suggest that BK postconditioning can promote neuronal autophagy in ROSC rats.

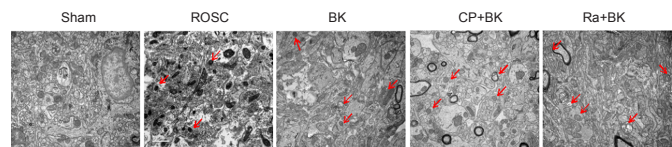


Figure 2 | Effect of bradykinin postconditioning on autophagosomes in the hippocampi of rats with restoration of spontaneous circulation, as detected by transmission electron microscopy.

Compared with the Sham group, the amount of neuronal autophagosomes in the ROSC group was increased. Compared with the ROSC group, the amount of neuronal autophagosomes in the BK group was increased. Compared with the BK group, the amount of neuronal autophagosomes in the CP + BK group remained unchanged, whereas in the Ra + BK group it was increased. Autophagosomes are indicated by red arrows. Scale bars: 1 μm. BK: Bradykinin; CP: compound C; Ra: rapamycin; ROSC: restoration of spontaneous circulation; Sham: sham operation.

Bradykinin postconditioning decreases apoptosis in the hippocampus of ROSC rats

The number of hippocampal TUNEL-positive cells was calculated to determine the effects of BK postconditioning on apoptosis in ROSC rats. As the TUNEL staining showed, the ROSC group exhibited significantly more hippocampal TUNEL-positive cells compared with the Sham group ($P < 0.01$). The BK group demonstrated a significant decrease in the number of hippocampal TUNEL-positive cells compared with the ROSC group ($P < 0.01$). The CP + BK group showed a significant increase in the number of hippocampal TUNEL-positive cells compared with the BK group ($P < 0.01$), while the Ra + BK group showed a significant decrease in the number of hippocampal TUNEL-positive cells compared with the BK group ($P < 0.01$; **Figure 3**). These findings suggest that BK postconditioning can reduce neuronal apoptosis in ROSC rats.

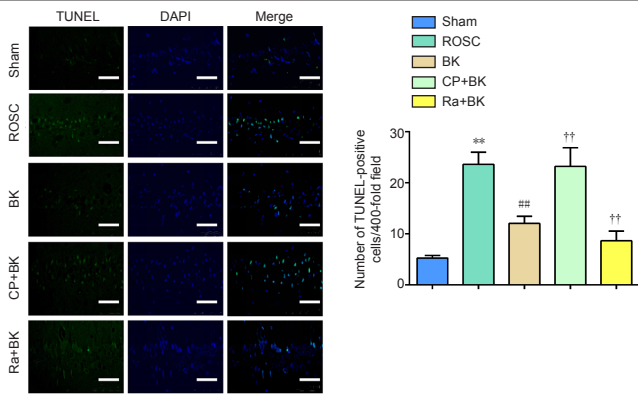


Figure 3 | Effect of bradykinin postconditioning on hippocampal cell apoptosis in rats with restoration of spontaneous circulation, as detected by terminal deoxynucleotidyl transferase dUTP nick end-labeling staining.

Compared with the Sham group, the number of TUNEL-positive cells in the ROSC group was significantly increased. Compared with the ROSC group, the number of TUNEL-positive cells in the BK group was significantly decreased. Compared with the BK group, the number of TUNEL-positive cells in the CP + BK group was significantly increased, while that in the Ra + BK group was significantly decreased. The normal cell nuclei are shown blue, while the TUNEL-positive cells (apoptotic cells) are shown in green. Scale bars: 50 μ m. All data are presented as the mean \pm SD ($n = 8$). ** $P < 0.01$, vs. Sham group; ### $P < 0.01$, vs. ROSC group; †† $P < 0.05$, vs. BK group (one-way analysis of variance followed by Tukey's *post hoc* test). BK: Bradykinin; CP: compound C; DAPI: 4',6-diamidino-2-phenylindole; Ra: rapamycin; ROSC: restoration of spontaneous circulation; Sham: sham operation; TUNEL: terminal deoxynucleotidyl transferase dUTP nick end labeling.

Bradykinin postconditioning affects the AMPK/mTOR signaling pathway, autophagy- and apoptosis-related proteins, and brain injury marker expression in the hippocampus of ROSC rats

Immunohistochemistry
The p-AMPK, p-mTOR, NBR1, p-62, LC3 and S100 β immunopositivity was measured to determine the effect of BK postconditioning on the AMPK/mTOR signaling pathway, autophagy-related proteins, and brain injury marker expression in ROSC rats. As shown in **Figure 4**, the rats in the ROSC group showed a significant decrease in p-mTOR and p62 immunopositivity (both $P < 0.01$), a significant increase in S100 β ($P < 0.01$), p-AMPK ($P < 0.05$), and LC3 ($P < 0.01$) immunopositivity, and no change in NBR1 immunopositivity ($P = 0.192$) compared with the Sham group. The BK group exhibited a significant decrease in p-mTOR, p62, and S100 β immunopositivity (all $P < 0.01$), as well as a significant increase in p-AMPK ($P < 0.05$), NBR1 ($P < 0.01$), and LC3 ($P < 0.01$) immunopositivity compared with the ROSC group. The CP + BK group showed a significant decrease in LC3 ($P < 0.01$), p-AMPK ($P < 0.01$), and NBR1 ($P < 0.05$) immunopositivity and a significant increase in S100 β , p62, and p-mTOR immunopositivity (all $P < 0.01$), while the Ra + BK group exhibited a significant increase in LC3 ($P < 0.01$), p-AMPK ($P < 0.01$), and NBR1 ($P < 0.05$) immunopositivity and a significant decrease in S100 β , p62 (both $P < 0.01$) and p-mTOR ($P < 0.05$) immunopositivity compared with the BK group. These findings suggest that BK postconditioning can inhibit S100 β expression in ROSC rat neurons, reduce nerve damage, activate the AMPK/mTOR signaling pathway, inhibit p62 expression, and increase the autophagy-related proteins NBR1 and LC3 expression to promote autophagy.

Western blot assay

The p-AMPK, p-mTOR and caspase-3 expression was measured to determine the effect of BK postconditioning on the AMPK/mTOR signaling pathway, and apoptosis-related protein expression in ROSC rats. As shown in **Figure 5**, the ROSC group exhibited a significant increase in p-AMPK and caspase-3 expression (both $P < 0.01$) and a significant decrease in p-mTOR expression ($P < 0.01$) compared with the Sham group. The BK group demonstrated a significant increase in p-AMPK expression ($P < 0.01$) and a significant decrease in p-mTOR and caspase-3 expression (both $P < 0.01$) compared with the ROSC group. The CP + BK group exhibited a significant decrease in p-AMPK expression ($P < 0.01$) and a significant increase in p-mTOR and caspase-3 expression (both $P < 0.01$), while the Ra + BK group exhibited a significant increase in p-AMPK and caspase-3 expression (both $P < 0.01$) and no significant changes in p-mTOR expression ($P = 0.26$) compared with the BK group. These findings suggest that BK postconditioning activates the AMPK/mTOR signaling pathway and inhibits caspase-3 expression.

Discussion

The kallikrein-kinin system mainly comprises the kinin, kininogen, kallikrein, and kinin-degrading enzymes. In mammals, it primarily includes BK, kallidin, and methionyl kallidin (Campbell, 2001). Kinins are a family of 9- to 11-amino-acid peptides that have similar biological functions (Talbot et al., 2013). The primary role of kininase is kinin degradation. There are two main groups of kininases: kininase I and kininase II. Kininase II can degrade BK, which produces inactive substances and causes BK to lose its biological function, whereas the angiotensin-converting enzyme inhibitor decreases BK degradation and enables it to accumulate locally to exert its biological effects (Kuoppala et al., 2000; Sharma and Al-Sherif, 2006; Hanif et al., 2010).

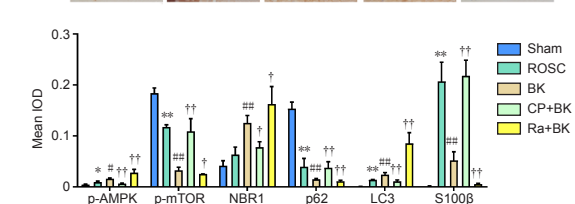
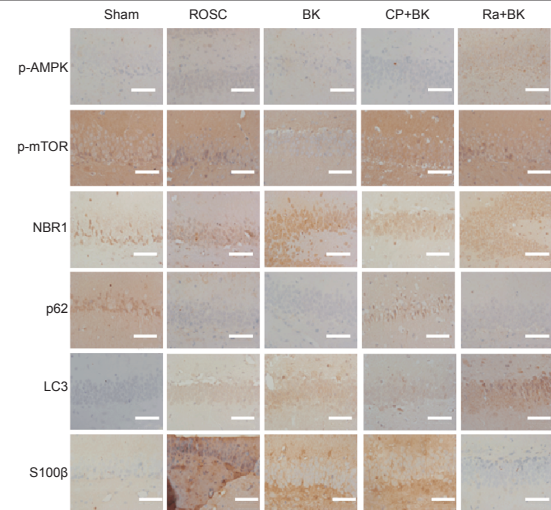


Figure 4 | Effect of bradykinin postconditioning on the immunopositivity of AMPK/mTOR signaling pathway, autophagy-related proteins, and brain injury marker in rats with restoration of spontaneous circulation, as detected by immunohistochemistry.

Compared with the Sham group, p-mTOR and p62 immunopositivity in the ROSC group was significantly decreased, S100 β , p-AMPK, and LC3 immunopositivity was significantly increased, and NBR1 immunopositivity remained unchanged. Compared with the ROSC group, p-mTOR, p62, and S100 β immunopositivity in the BK group was significantly decreased, while p-AMPK, NBR1, and LC3 immunopositivity was significantly increased. Compared with the BK group, LC3, p-AMPK, and NBR1 immunopositivity in the CP+BK group was significantly decreased, whereas S100 β , p62, and p-mTOR immunopositivity was significantly increased; LC3, p-AMPK, and NBR1 immunopositivity in the Ra+BK group was significantly increased, while S100 β , p62, and p-mTOR immunopositivity was significantly decreased. Scale bars: 50 μ m. All data are presented as the mean \pm SD ($n = 8$). * $P < 0.05$, ** $P < 0.01$, vs. Sham group; # $P < 0.05$, ### $P < 0.01$, vs. ROSC group; † $P < 0.05$, †† $P < 0.01$, vs. BK group (one-way analysis of variance followed by Tukey's *post hoc* test). BK: Bradykinin; CP: compound C; IOD: integrated optical density; LC3: microtubule-associated protein 1 light chain 3; NBR1: neighbor of breast cancer 1 gene; p-AMPK: phosphorylated adenosine-monophosphate activated protein kinase; p-mTOR: p-mechanistic target of rapamycin; Ra: rapamycin; ROSC: restoration of spontaneous circulation; S100 β : S100 calcium-binding protein B; Sham: sham operation.

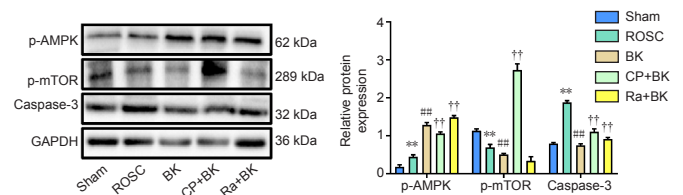


Figure 5 | Effect of bradykinin postconditioning on the AMPK/mTOR signaling pathway and apoptosis-related protein expression in rats with restoration of spontaneous circulation, as detected by western blot.

Original images of bands were shown in Additional Figure 2. All data are presented as the mean \pm SD ($n = 8$). ** $P < 0.01$, vs. Sham group; ### $P < 0.01$, vs. ROSC group; †† $P < 0.01$, vs. BK group (one-way analysis of variance followed by Tukey's *post hoc* test). BK: Bradykinin; caspase-3: cysteine-aspartic acid proteases; CP: compound C; GAPDH: glyceraldehyde 3-phosphate dehydrogenase; p-AMPK: phosphorylated adenosine monophosphate-activated protein kinase; p-mTOR: phosphorylated mechanistic target of rapamycin; Ra: rapamycin; ROSC: restoration of spontaneous circulation; Sham: sham operation.

The retention time of BK in the body is short, usually only a few minutes, and its half-life in plasma is approximately 30 seconds (Cyr et al., 2001; Bork et al., 2007). Previous studies found that BK exerts its biological function through the B1 receptor and B2R, particularly B2R, which plays a vital role in the cardiovascular system (Regoli et al., 1994; Cloutier et al., 2004; Dagher et al., 2019). It most likely affects cardiomyocytes by stimulating B2R on the vascular endothelial cell membrane to produce nitric oxide active substance; alternatively, it may directly bind B2R on cardiomyocytes to enhance the production of the second messenger inositol 1,4,5-trisphosphate. Following a series of signaling steps, nitric oxide is produced, which ultimately protects cardiomyocytes from oxidative stress-induced senescence (Dong et al., 2013; Fu et al., 2015). BK is related to the potential of cardiac endothelial angiogenesis (Nurmi et al., 2012). Therefore, BK plays an important role

in cardiovascular disease, for example by reducing myocardial ischemia-reperfusion injury, affecting cardiac remodeling, delaying heart failure, and delaying vascular endothelial senescence (Yeh et al., 2010).

In the current study, we evaluated the neuroprotective effect of BK postconditioning on neurons in a rat model of ROSC after CA. Behavioral assessment showed that BK postconditioning improved NDS in ROSC rats. The TUNEL results demonstrated that BK postconditioning reduced neuronal apoptosis in ROSC rats. Immunohistochemistry analysis showed that BK postconditioning inhibited the expression of S100 β , which is a nerve tissue protein (He et al., 2018), in the neurons of ROSC rats. When brain tissue is damaged, S100 β levels increase in the cerebrospinal fluid; thus, S100 β is a marker of blood-cerebrospinal fluid barrier injury. When its levels increase, this indicates that severe brain injury may have occurred (Hafez and El-Sarnagawy, 2020). The findings from this study suggest that BK postconditioning can significantly reduce neuronal injury in ROSC rats.

ROSC after CPR can cause ischemia-reperfusion injury to the brain. Cerebral ischemia directly injures neurons, and reperfusion also induces neuronal damage. The pathophysiological mechanism is primarily associated with signaling pathway activation that leads to the formation of oxygen free radicals, excitotoxic injury induced by glutamate release, calcium homeostasis imbalance, and cell death (Hopper et al., 2014; Videla-Richardson et al., 2019; Wang et al., 2019). Neurological dysfunction can occur if a large number of neurons are damaged. In severe cases, coma, persistent vegetative state, and even death may occur (Elmer and Callaway, 2017). Apoptosis, necrosis, and autophagy are the histological manifestations of neuronal death, and they interact with and restrict each other, thereby determining cell fate (Zille et al., 2017; Chi et al., 2018; Xu et al., 2018).

Autophagy was first observed in hepatocytes by electron microscopy in 1962. It is also known as "type II programmed cell death" (Ashford and Porter, 1962). During autophagy, lysosomes degrade senescent, denatured, and damaged organelles or macromolecules. This biological phenomenon is specific to eukaryotes and plays an important role in cell proliferation, differentiation, development, homeostasis, and survival. Studies have illustrated that autophagy is activated in models of ischemia-hypoxia, global or regional cerebral ischemia brain injury, and has a two-way regulatory effect on cell fate that depend on the cell type and stimuli (Au et al., 2015; Wang et al., 2019). Appropriate autophagy can promote neuronal survival, while excessive autophagy causes cell death (Hou et al., 2019; Stavoe and Holzbaur, 2019). Tao et al. (2018) found that neuronal autophagy is activated in a rat model of brain injury and plays an important role in nerve tissue repair. Cui et al. (2016) reported that autophagy activation in a CA animal model mediates hippocampal neuronal death in the later stage of ROSC after CPR. However, a previous study by Zeng et al. (2013) suggested that autophagy is reduced in rats that undergo CPR after CA, and that enhancing autophagy could inhibit neuronal injury. Our study found that the amount of autophagosomes in rat brain tissue and the IOD value of the autophagy-related protein LC3 were increased, and the p62 expression was downregulated, indicating that the level of autophagy was increased after ROSC, which is consistent with the study by Cui et al. (2016).

Autophagy is regulated by various signaling pathways. When cells are ischemic and subjected to energy depletion, they are regulated by autophagy, which is primarily activated via the sirtuin 1/forkhead box protein O1 and AMPK pathways (Miyachi et al., 2019; Xu et al., 2020). AMPK is an important ATP/AMP energy sensor protein and regulator of energy metabolism (Hinchy et al., 2018), and is widely expressed in the central nervous system and peripheral tissues (Villanueva-Paz et al., 2016; Herzig and Shaw, 2018; Li and Chen, 2019). In response to stress, ischemia, hypoxia, strenuous exercise, decreased ATP levels, and increased intracellular AMP levels, AMPK is activated to regulate downstream pathways, which increases ATP levels in the body to maintain the balance of cell energy metabolism and promote cell survival. Therefore, AMPK act as a central node for cells to balance energy demands (Carling, 2017; Herzig and Shaw, 2018). AMPK is used to treat metabolic diseases, such as obesity, diabetes, inflammation, and cancer (Jeon, 2016; Wang et al., 2016). mTOR is a protein that belongs to the phosphatidylinositol 3-kinase-related kinase family. It is an atypical serine/threonine kinase that plays a role in mTOR complex1 and 2 formation. Studies have found that AMPK activates and phosphorylates Unc-51-like autophagy activating kinase 1 and promotes the autophagy cascade, whereas mTOR suppresses autophagy by inhibiting Unc-51-like autophagy activating kinase 1 (Kim et al., 2011; Gui et al., 2017; Liu et al., 2018). Therefore, AMPK affects the level of autophagy by negatively regulating mTOR expression via the Unc-51-like autophagy activating kinase 1 node (Kim et al., 2011). Studies have shown that AMPK/mTOR signaling-mediated autophagy is protective in myocardial ischemia (Yang et al., 2013) and that mTOR inhibition is protective in cerebral ischemia via autophagy initiation (Wang et al., 2012; Srivastava et al., 2016).

He et al. (2020) reported increases in the level of autophagy and in particular in the rate of apoptosis and downregulation in p-AMPK expression in the brain tissue of mice undergoing CPR after CA. Treatment with adiponectin stimulates autophagy and inhibits apoptosis, thereby protecting mouse brain. Zhu et al. (2018) also found that, after ROSC following CA and CPR, pretreatment with metformin induced autophagy, which was accompanied by AMPK phosphorylation, whereas AMPK or autophagy inhibitors eliminated the neuroprotective effects of AMPK, demonstrating that AMPK activation plays a key function in the increase in autophagy. Therefore, in the current study, BK, combined with the AMPK inhibitor CP and the autophagy activator Ra, was used to treat rats that underwent CPR after CA. The expression of

autophagy-related proteins (LC3, NBR1, and p62), brain injury marker (S100 β) proteins involved in related pathways (p-AMPK and p-mTOR), and apoptosis-related protein (caspase-3) was assessed. The immunohistochemistry and western blotting results showed that BK postconditioning significantly increased autophagy, upregulated NBR1 and LC3 expression, and downregulated p62, caspase-3 and S100 β expressions in our rat model. In addition, these treatment conditions promoted AMPK phosphorylation and inhibited mTOR phosphorylation. The addition of CP inhibited, while the addition of Ra promoted, the aforementioned effects of BK. Therefore, these results indicated that, through AMPK/mTOR signaling pathway activation, BK can promote autophagy, inhibit apoptosis, and prevent the brain injury induced by ROSC after CA. Ra was used to evaluate the enhancement of the protective effect of autophagy on neurons in the rat model. The behavioral assessment demonstrated a significant increase in NDS of rats in the Ra + BK group compared with that in the BK group, suggesting that Ra enhanced the protective effect of BK on the rat model.

Comparison with treatment using Ra or CP alone was not performed in this study because this study primarily addressed the protective effects of BK treatment on the hippocampal neurons of SD rats after ROSC. Ra and CP were mainly used to explore the effects of BK on the AMPK/mTOR signaling pathway. Treatment with Ra or CP alone has no significant role in the study of the mechanism of BK, and it is indeed not necessary to eliminate the interference effect here. It is not essential to demonstrate the effects of Ra and CP alone on the rat model, because the combined action of BK with Ra or CP can prove the relationship between BK and the AMPK/mTOR signaling pathway, or the combined effect of BK with Ra or CP on autophagy in rats after ROSC.

A limitation of the present study is that the mechanism by which BK regulates autophagy was not studied in detail, for example how BK regulates the AMPK/mTOR signaling pathway, if there are other regulatory pathways, and whether BK acts through B1 or B2 receptors. Future studies should explore these aspects, as well as the degree of phosphorylation, the relationship between the autophagy-related proteins, and caspase-3 activation.

In summary, neuronal autophagy levels and apoptosis rates were increased in rats after ROSC from CA. BK postconditioning increased neuronal autophagy levels and inhibited apoptosis, thus reducing the degree of brain injury caused by ROSC after CA, and this effect was mediated by activation of the AMPK/mTOR signaling pathway.

Author contributions: Study design and conception: SRL, BS, FC; experiment implementation, data collection and analysis: SRL, BS, QML, YJL, XQ, XPW, ZG; data interpretation: SRL, BS, QML, YJL, FC; manuscript draft: SRL, BS. All authors read and approved the final manuscript.

Conflicts of interest: The authors declare that there is no conflict of interests.

Availability of data and materials: All data generated or analyzed during this study are included in this published article and its supplementary information files.

Open access statement: This is an open access journal, and articles are distributed under the terms of the Creative Commons AttributionNonCommercial-ShareAlike 4.0 License, which allows others to remix, tweak, and build upon the work non-commercially, as long as appropriate credit is given and the new creations are licensed under the identical terms.

Open peer reviewer: Henning Solange Rodrigues Ulrich, University of Sao Paulo, Brazil.

Additional files:

Additional Figure 1: Establishment of cardiac arrest rat model.

Additional Figure 2: The original images of p-AMPK (A), p-mTOR (B), caspase-3 (C), and GAPDH (D) by western blot assay.

Additional Table 1: Scoring criteria of neurological deficit scale.

Additional file 1: Open peer review report 1.

References

- Abelairas-Gómez C, Tipton MJ, González-Salvado V, Bierens J (2019) Drowning: epidemiology, prevention, pathophysiology, resuscitation, and hospital treatment. *Emergencias* 31:270-280.
- Andersen LW, Holmberg MJ, Berg KM, Donnino MW, Granfeldt A (2019) In-hospital cardiac arrest: a review. *JAMA* 321:1200-1210.
- Ashford TP, Porter KR (1962) Cytoplasmic components in hepatic cell lysosomes. *J Cell Biol* 12:198-202.
- Au AK, Chen Y, Du L, Smith CM, Manole MD, Baltagi SA, Chu CT, Aneja RK, Bayir H, Kochanek PM, Clark RS (2015) Ischemia-induced autophagy contributes to neurodegeneration in cerebellar Purkinje cells in the developing rat brain and in primary cortical neurons in vitro. *Biochim Biophys Acta* 1852:1902-1911.
- Bork K, Frank J, Grundt B, Schlattmann P, Nussberger J, Kreuz W (2007) Treatment of acute edema attacks in hereditary angioedema with a bradykinin receptor-2 antagonist (Icatibant). *J Allergy Clin Immunol* 119:1497-1503.
- Campbell DJ (2001) The kallikrein-kinin system in humans. *Clin Exp Pharmacol Physiol* 28:1060-1065.
- Carling D (2017) AMPK signalling in health and disease. *Curr Opin Cell Biol* 45:31-37.
- Chi H, Chang HY, Sang TK (2018) Neuronal cell death mechanisms in major neurodegenerative diseases. *Int J Mol Sci* 19:3082.
- Cloutier F, Ongali B, Campos MM, Thibault G, Neugebauer W, Couture R (2004) Correlation between brain bradykinin receptor binding sites and cardiovascular function in young and adult spontaneously hypertensive rats. *Br J Pharmacol* 142:285-296.

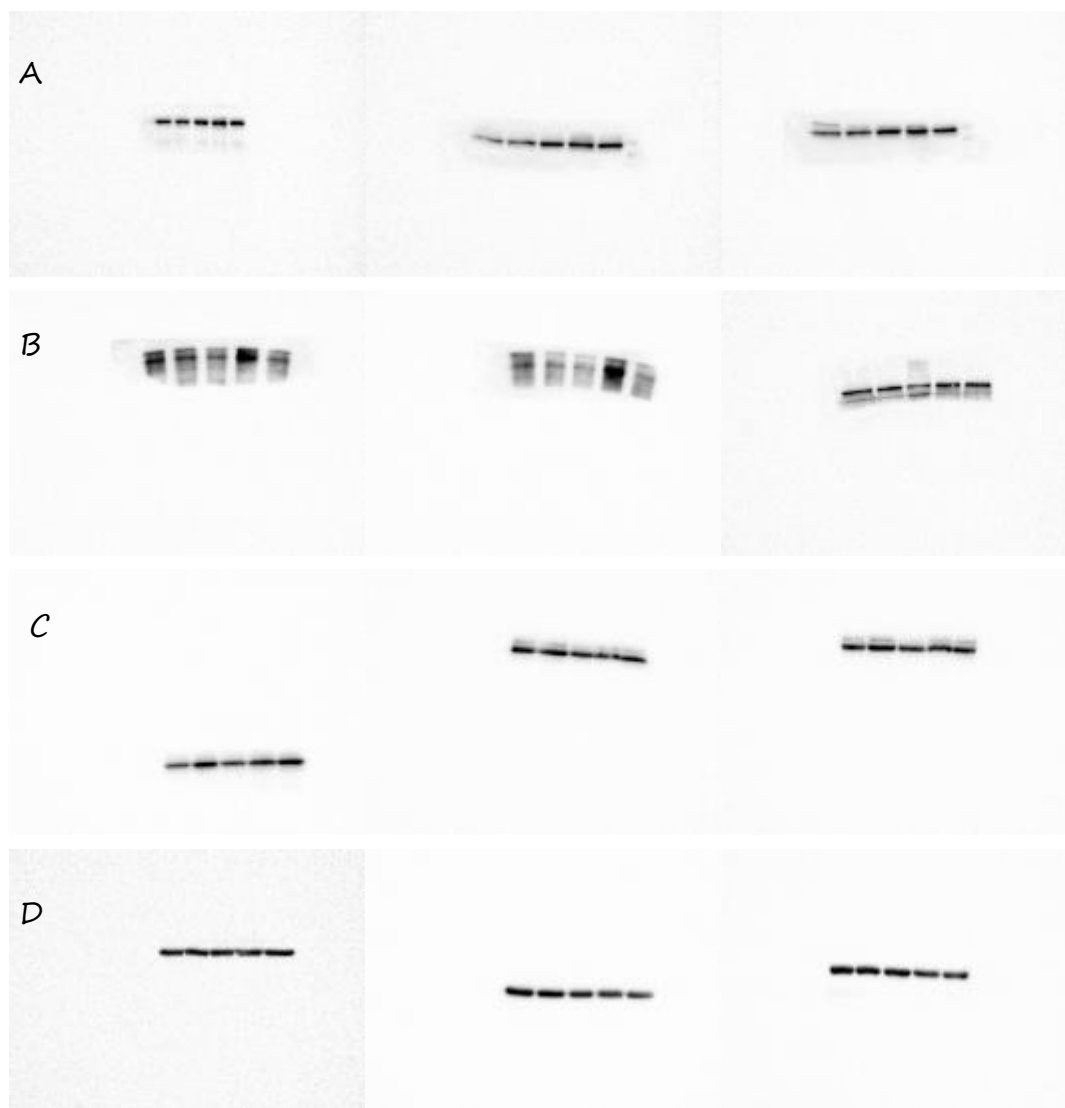
- Cui D, Shang H, Zhang X, Jiang W, Jia X (2016) Cardiac arrest triggers hippocampal neuronal death through autophagic and apoptotic pathways. *Sci Rep* 6:27642.
- Cyr M, Lepage Y, Blais C, Jr., Gervais N, Cugno M, Rouleau JL, Adam A (2001) Bradykinin and des-Arg(9)-bradykinin metabolic pathways and kinetics of activation of human plasma. *Am J Physiol Heart Circ Physiol* 281:H275-283.
- Dagher OK, Jaffa MA, Habib A, Ziyadeh FN, Jaffa AA (2019) Heteromerization fingerprints between bradykinin B2 and thromboxane TP receptors in native cells. *PLoS One* 14:e0216908.
- Danielisová V, Gottlieb M, Némethová M, Kravčuková P, Domoráková I, Mečířová E, Burda J (2009) Bradykinin postconditioning protects pyramidal CA1 neurons against delayed neuronal death in rat hippocampus. *Cell Mol Neurobiol* 29:871-878.
- Dong R, Xu X, Li G, Feng W, Zhao G, Zhao J, Wang DW, Tu L (2013) Bradykinin inhibits oxidative stress-induced cardiomyocytes senescence via regulating redox state. *PLoS One* 8:e77034.
- Elmer J, Callaway CW (2017) The brain after cardiac arrest. *Semin Neurol* 37:19-24.
- Fu C, Li B, Sun Y, Ma G, Yao Y (2015) Bradykinin inhibits oxidative stress-induced senescence of endothelial progenitor cells through the B2R/AKT/RB and B2R/EGFR/RB signal pathways. *Oncotarget* 6:24675-24689.
- Gao QS, Zhang YH, Xue H, Wu ZY, Li C, Zhao P (2021) Brief inhalation of sevoflurane can reduce glial scar formation after hypoxic-ischemic brain injury in neonatal rats. *Neural Regen Res* 16:1052-1061.
- Geocadin RG, Muthuswamy J, Sherman DL, Thakor NV, Hanley DF (2000) Early electrophysiological and histologic changes after global cerebral ischemia in rats. *Mov Disord* 15 Suppl 1:14-21.
- Goebel U, Scheid S, Spassov S, Schallner N, Wollborn J, Buerkle H, Ulbrich F (2021) Argon reduces microglial activation and inflammatory cytokine expression in retinal ischemia/reperfusion injury. *Neural Regen Res* 16:192-198.
- Gui D, Cui Z, Zhang L, Yu C, Yao D, Xu M, Chen M, Wu P, Li G, Wang L, Huang X (2017) Salidroside attenuates hypoxia-induced pulmonary arterial smooth muscle cell proliferation and apoptosis resistance by upregulating autophagy through the AMPK-mTOR-ULK1 pathway. *BMC Pulm Med* 17:191.
- Gunaruwan P, Maher A, Williams L, Sharman J, Schmitt M, Campbell R, Frenneau M (2009) Effects of bradykinin on venous capacitance in health and treated chronic heart failure. *Clin Sci (Lond)* 116:443-450.
- Hafez AS, El-Sarnagawy GN (2020) S-100 β in predicting the need of hyperbaric oxygen in CO-induced delayed neurological sequels. *Hum Exp Toxicol* 39:614-623.
- Hanif K, Bid HK, Konwar R (2010) Reinvesting the ACE inhibitors: some old and new implications of ACE inhibition. *Hypertens Res* 33:11-21.
- Hao M, Zhu S, Hu L, Zhu H, Wu X, Li Q (2017) Myocardial ischemic postconditioning promotes autophagy against ischemia reperfusion injury via the activation of the nNOS/AMPK/mTOR pathway. *Int J Mol Sci* 18:614.
- He JY, Wang J, Guan YQ, Tian X, Liao QJ, Qin J (2011) The effect of insulin on the expressions of Bcl-2, Bax mRNA and hippocampus neuronal apoptosis in rats after cardiopulmonary resuscitation. *Zhonghua Jizhen Yixue Zazhi* 20:1056-1061.
- He Y, Cai Z, Chen Y (2018) Role of S-100 β in stroke. *Int J Neurosci* 128:1180-1187.
- He Y, Liu B, Yao P, Shao Y, Cheng Y, Zhao J, Wu J, Zhao ZW, Huang W, Christopher TA, Lopez B, Ma X, Cao X (2020) Adiponectin inhibits cardiac arrest/cardiopulmonary resuscitation-induced apoptosis in brain by increasing autophagy involved in adipor1-AMPK signaling. *Mol Med Res* 22:870-878.
- Herzig S, Shaw RJ (2018) AMPK: guardian of metabolism and mitochondrial homeostasis. *Nat Rev Mol Cell Biol* 19:121-135.
- Hinchey EC, Gruszczak AV, Willows R, Navaratnam N, Hall AR, Bates G, Bright TP, Krieg T, Carling D, Murphy MP (2018) Mitochondria-derived ROS activate AMP-activated protein kinase (AMPK) indirectly. *J Biol Chem* 293:17208-17217.
- Hopper K, Borchers A, Epstein SE (2014) Acid base, electrolyte, glucose, and lactate values during cardiopulmonary resuscitation in dogs and cats. *J Vet Emerg Crit Care (San Antonio)* 24:208-214.
- Hou K, Xu D, Li F, Chen S, Li Y (2019) The progress of neuronal autophagy in cerebral ischemia stroke: Mechanisms, roles and research methods. *J Neurol Sci* 400:72-82.
- Jeon SM (2016) Regulation and function of AMPK in physiology and diseases. *Exp Mol Med* 48:e245.
- Jia X, Koenig MA, Shin HC, Zhen G, Yamashita S, Thakor NV, Geocadin RG (2006) Quantitative EEG and neurological recovery with therapeutic hypothermia after asphyxial cardiac arrest in rats. *Brain Res* 1111:166-175.
- Kim J, Kundu M, Viollet B, Guan KL (2011) AMPK and mTOR regulate autophagy through direct phosphorylation of Ulk1. *Nat Cell Biol* 13:132-141.
- Kuoppala A, Lindstedt KA, Saarinen J, Kovanen PT, Kokkonen JO (2000) Inactivation of bradykinin by angiotensin-converting enzyme and by carboxypeptidase N in human plasma. *Am J Physiol Heart Circ Physiol* 278:H1069-1074.
- Lee JC, Tae HJ, Cho JH, Kim IS, Lee TK, Park CW, Park YE, Ahn JH, Park JH, Yan BC, Lee HA, Hong S, Won MH (2019) Therapeutic hypothermia attenuates paraplegia and neuronal damage in the lumbar spinal cord in a rat model of asphyxial cardiac arrest. *J Therm Biol* 83:1-7.
- Li Y, Chen Y (2019) AMPK and Autophagy. *Adv Exp Med Biol* 1206:85-108.
- Lin QM, Tang XH, Lin SR, Chen BD, Chen F (2020) Bone marrow-derived mesenchymal stem cell transplantation attenuates overexpression of inflammatory mediators in rat brain after cardiopulmonary resuscitation. *Neural Regen Res* 15:324-331.
- Lin S, Song B, Lin Q, Qian X, Ke J, Wang X, Chen M, Chen F (2015) Protective effect of bradykinin postconditioning on neurons in rats following cardiopulmonary resuscitation. *Zhonghua Jizhen Yixue Zazhi* 24:969-974.
- Liu B, Tu Y, He W, Liu Y, Wu W, Fang Q, Tang H, Tang R, Wan Z, Sun W, Wan Y (2018) Hyperisoleucine attenuates renal aging and injury induced by D-galactose via inhibiting AMPK-ULK1 signaling-mediated autophagy. *Aging (Albany NY)* 10:4197-4212.
- Liu Y, Lu Z, Cui M, Yang Q, Tang Y, Dong Q (2016) Tissue kallikrein protects SH-SY5Y neuronal cells against oxygen and glucose deprivation-induced injury through bradykinin B2 receptor-dependent regulation of autophagy induction. *J Neurochem* 139:208-220.
- Lu L, Lian Y, Xu S, Yu Z (2020) Comparison of brain injuries in rat cardiac arrest models induced by asphyxia and electrical stimulation. *Zhonghua Wei Zhong Bing Ji Jiu Yi Xue* 32:336-340.
- Martins AH, Alves JM, Perez D, Carrasco M, Torres-Rivera W, Eterović VA, Ferchmin PA, Ulrich H (2012) Kinin-B2 receptor mediated neuroprotection after NMDA excitotoxicity is reversed in the presence of kinin-B1 receptor agonists. *PLoS One* 7:e30755.
- Miyauchi T, Uchida Y, Kadono K, Hirao H, Kawasoe J, Watanabe T, Ueda S, Okajima H, Terajima H, Uemoto S (2019) Up-regulation of FOXO1 and reduced inflammation by β -hydroxybutyric acid are essential diet restriction benefits against liver injury. *Proc Natl Acad Sci U S A* 116:13533-13542.
- Nolan JP (2017) Cardiac Arrest and Cardiopulmonary Resuscitation. *Semin Neurol* 37:5-12.
- Nurmi L, Heikkilä HM, Vapaatalo H, Kovanen PT, Lindstedt KA (2012) Downregulation of bradykinin type 2 receptor expression in cardiac endothelial cells during senescence. *J Vasc Res* 49:13-23.
- Olson TP, Frantz RP, Turner ST, Bailey KR, Wood CM, Johnson BD (2009) Gene variant of the bradykinin B2 receptor influences pulmonary arterial pressures in heart failure patients. *Clin Med Circ Respir Pulm Med* 2009:9-17.
- Paterson KJ, Zambreanu L, Bennett DL, McMahon SB (2013) Characterisation and mechanisms of bradykinin-evoked pain in man using iontophoresis. *Pain* 154:782-792.
- Percie du Sert N, Hurst V, Ahluwalia A, Alam S, Avey MT, Baker M, Browne WJ, Clark A, Cuthill IC, Dirnagl U, Emerson M, Garner P, Holgate ST, Howells DW, Karp NA, Lazic SE, Lidster K, MacCallum CJ, Macleod M, Pearl EJ, et al. (2020) The ARRIVE guidelines 2.0: Updated guidelines for reporting animal research. *PLoS Biol* 18:e3000410.
- Perman SM, Stanton E, Soar J, Berg RA, Donnino MW, Mikkelsen ME, Edelson DP, Churpek MM, Yang L, Merchant RM; American Heart Association's Get With the Guidelines[®]—Resuscitation (formerly the National Registry of Cardiopulmonary Resuscitation) Investigators (2016) Location of In-Hospital Cardiac Arrest in the United States-Variability in Event Rate and Outcomes. *J Am Heart Assoc* 5:e003638.
- Qu Z, Xu H, Tian Y (2015) Effects of angiotensin-converting enzyme inhibition and bradykinin peptides in rats with myocardial infarction. *Int J Clin Exp Pathol* 8:3410-3417.
- Radeschi G, Mina A, Berta G, Fasiola A, Roasio A, Urso F, Penso R, Zumbo U, Berchiolla P, Ristagno G, Sandroni C, Piedmont IHCA Registry Initiative (2017) Incidence and outcome of in-hospital cardiac arrest in Italy: a multicentre observational study in the Piedmont Region. *Resuscitation* 119:48-55.
- Regoli D, Gobeil F, Nguyen QT, Jukic D, Seoane PR, Salvino JM, Sawutz DG (1994) Bradykinin receptor types and B2 subtypes. *Life Sci* 55:735-749.
- Roman-Campos D, Duarte HL, Gomes ER, Castro CH, Guatimosim S, Natali AJ, Almeida AP, Pesquero JB, Pesquero JL, Cruz JS (2010) Investigation of the cardiomyocyte dysfunction in bradykinin type 2 receptor knockout mice. *Life Sci* 87:715-723.
- Sharma JN (2009) Hypertension and the bradykinin system. *Curr Hypertens Rep* 11:178-181.
- Sharma JN, Al-Sherif GJ (2006) Pharmacologic targets and prototype therapeutics in the kallikrein-kinin system: bradykinin receptor agonists or antagonists. *ScientificWorldJournal* 6:1247-1261.
- Singh P, Krishna A, Sridaran R (2011) Changes in bradykinin and bradykinin B(2)-receptor during estrous cycle of mouse. *Acta Histochem* 113:436-441.
- Srivastava IN, Shperdheja J, Baybis M, Ferguson T, Crino PB (2016) mTOR pathway inhibition prevents neuroinflammation and neuronal death in a mouse model of cerebral palsy. *Neurobiol Dis* 85:144-154.
- Stavoe AKH, Holzbaur ELF (2019) Autophagy in neurons. *Annu Rev Cell Dev Biol* 35:477-500.
- Talbot S, Lin JC, Couture R (2013) Chapter 207. Kinin receptors. In: *Handbook of biologically active peptides*, 2nd Edition (Kastin AJ, ed). Cambridge, MA, USA: Academic Press Inc.
- Tao J, Shen C, Sun Y, Chen W, Yan G (2018) Neuroprotective effects of pinocembrin on ischemia/reperfusion-induced brain injury by inhibiting autophagy. *Biomed Pharmacother* 106:1003-1010.
- Twhogh CJ, Singer B, Grier G, Finney SJ (2019) A systematic literature review and meta-analysis of the effectiveness of extracorporeal-CPR versus conventional-CPR for adult patients in cardiac arrest. *J Intensive Care Soc* 20:347-357.
- Videla-Richardson GA, Furmento VA, Garcia CP, Morris-Hanon O, Sevelev GE, Romorini L, Scassa ME (2019) Human embryonic stem cells display a pronounced sensitivity to the cyclin dependent kinase inhibitor Roscovitine. *BMC Mol Cell Biol* 20:40.
- Villanueva-Paz M, Cotán D, Garrido-Maraver J, Oropesa-Ávila M, de la Mata M, Delgado-Pavón A, de Laveria I, Alcocer-Gómez E, Álvarez-Córdoba M, Sánchez-Alcázar JA (2016) AMPK Regulation of Cell Growth, Apoptosis, Autophagy, and Bioenergetics. *Exp Suppl* 107:45-71.
- Vinten-Johansen J, Zhao ZQ, Zatta AJ, Kin H, Halkos ME, Kerendi F (2005) Postconditioning—A new link in nature's armor against myocardial ischemia-reperfusion injury. *Basic Res Cardiol* 100:295-310.
- Viryph PA, Shelyuk OV, Kabanova TA, Khalimova EI, Martynuk VS, Pavlovsky VI, Andronati SA (2017) Effect of 3-substituted 1,4-benzodiazepin-2-ones on bradykinin-induced smooth muscle contraction. *Ukr Biochem J* 89:31-37.
- Wallmuller C, Meron G, Kurkciyan I, Schober A, Stratil P, Sterz F (2012) Causes of in-hospital cardiac arrest and influence on outcome. *Resuscitation* 83:1206-1211.
- Wang P, Guan YF, Du H, Zhai QW, Su DF, Miao CY (2012) Induction of autophagy contributes to the neuroprotection of nicotinamide phosphoribosyltransferase in cerebral ischemia. *Autophagy* 8:77-87.
- Wang X, Sun D, Hu Y, Xu X, Jiang W, Shang H, Cui D (2019) The roles of oxidative stress and Beclin-1 in the autophagosome clearance impairment triggered by cardiac arrest. *Free Radic Biol Med* 136:87-95.
- Wang Z, Wang N, Liu P, Xie X (2016) AMPK and Cancer. *Exp Suppl* 107:203-226.
- Xu C, Wang L, Fozouni P, Evjen G, Chandra V, Jiang J, Lu C, Nicastrini M, Bretz C, Winkler JD, Amaravadi R, Garcia BA, Adams PD, Ott M, Tong W, Johansen T, Dou Z, Berger SL (2020) SIRT1 is downregulated by autophagy in senescence and ageing. *Nat Cell Biol* 22:1170-1179.
- Xu L, Shen J, McQuillan PM, Hu Z (2018) Anesthetic agents and neuronal autophagy. *What We Know and What We Don't*. *Curr Med Chem* 25:908-916.
- Yang K, Xu C, Li X, Jiang H (2013) Combination of D942 with curcumin protects cardiomyocytes from ischemic damage through promoting autophagy. *J Cardiovasc Pharmacol Ther* 18:570-581.
- Yang XM, Proctor JB, Cui L, Krieg T, Downey JM, Cohen MV (2004) Multiple, brief coronary occlusions during early reperfusion protect rabbit hearts by targeting cell signaling pathways. *J Am Coll Cardiol* 44:1103-1110.
- Yeh CH, Chen TP, Wang YC, Lin YM, Fang SW (2010) Cardiomyocyte apoptosis limited by bradykinin via restoration of nitric oxide after cardioplegic arrest. *J Surg Res* 163:e1-9.
- Zeng XY, Xiong HX, Li X, Xia JM, Wei HY, Liao XX, Hu CL, Jin XL (2013) Activation of autophagy improves neuron injury after the restoration of spontaneous circulation from ventricular fibrillation in wistar rats. *Zhonghua Jizhen Yixue Zazhi* 22:1327-1332.
- Zhao ZQ, Vinten-Johansen J (2006) Postconditioning: reduction of reperfusion-induced injury. *Cardiovasc Res* 70:200-211.
- Zhao ZQ, Corvera JS, Halkos ME, Kerendi F, Wang NP, Guyton RA, Vinten-Johansen J (2003) Inhibition of myocardial injury by ischemic postconditioning during reperfusion: comparison with ischemic preconditioning. *Am J Physiol Heart Circ Physiol* 285:H579-588.
- Zhu J, Liu K, Huang K, Gu Y, Hu Y, Pan S, Ji Z (2018) Metformin improves neurologic outcome via amp-activated protein kinase-mediated autophagy activation in a rat model of cardiac arrest and resuscitation. *J Am Heart Assoc* 7:e008389.
- Zille M, Karuppagounder SS, Chen Y, Gough PJ, Bertin J, Finger J, Milner TA, Jonas EA, Ratan RR (2017) Neuronal death after hemorrhagic stroke in vitro and in vivo shares features of ferroptosis and necroptosis. *Stroke* 48:1033-1043.

C-Editor: Zhao M; S-Editors: Yu J, Li CH; L-Editors: Crow M, Song LP; T-Editor: Jia Y



Additional Figure 1 Establishment of cardiac arrest rat model.

(A) Under anesthesia, the catheter was inserted into the trachea. (B) The left femoral artery was separated, the blood flow was blocked with ophthalmic forceps, and the distal end was ligated.



Additional Figure 2 The original images of p-AMPK (A), p-mTOR (B), caspase-3 (C), and GAPDH (D) by western blot assay.

GAPDH: glyceraldehyde 3-phosphate dehydrogenase; p-AMPK: phosphorylated adenosine monophosphate activated protein kinase; p-mTOR: phosphorylated mechanistic target of rapamycin.

Additional Table 1 Scoring criteria of neurological deficit scale

Item	Scoring criteria
(A) General behaviour	Total score = 19
1. State of consciousness	Normal (10), drowsiness (5), coma (0)
2. State of wakefulness	Spontaneous eye opening (3), eye opening in response to pain (1), no eye opening (0)
3. Respiratory state	Normal (6), abnormal (1), absent (0)
(B) Brainstem reflex	Total score = 21
1. Olfactory sensation	Present (3), absent (0)
2. Visual sensation	Present (3), absent (0)
3. Pupillary reflex	Present (3), absent (0)
4. Corneal reflex	Present (3), absent (0)
5. Startle reflex	Present (3), absent (0)
6. Beard tactile reflex	Present (3), absent (0)
7. Swallowing reflex	Present (3), absent (0)
(C) Movement	Total score = 6
Strength (left and right tested and scored respectively)	Normal (3), stiffness or weakness (1), no movement/paralysis (0)
(D) Sensory	Total score = 6
Pain (left and right tested and scored respectively)	Rapid avoidance of pain stimuli (3), weak or abnormal response (1), no avoidance response (0)
(E) Motor	Total score = 6
1. Gait coordination	Normal (3), abnormal (1), absent (0)
2. Balance ability	Normal (3), abnormal (1), absent (0)
(F) Behavior	Total score = 12
1. Righting reflex	Normal (3), abnormal (1), absent (0)
2. Negative geotaxis reflex	Normal (3), abnormal (1), absent (0)
3. Visual positioning	Normal (3), abnormal (1), absent (0)
4. Steering test	Normal (3), abnormal (1), absent (0)
(G) Seizures	Total score = 10
	No seizures (10), focal seizures, (5), generalized seizures (0)